Silikáty 33, s. 105—122 (1989)

THE MAIN TECHNOLOGICAL CHARACTERISTICS OF GLASS MELTING ZONES WITH RESPECT TO THE COURSE OF THE MELTING PROCESS

PART III. THE MAIN CHARACTERISTICS HOLDING TILL COMPLETE SAND DISSOLUTION AND REFINING

LUBOMÍR NĚMEC, SIMONA LAURENTOVÁ*)

Institute of the Chemistry of Glass and Ceramics, Czechoslovak Academy of Sciences, Lípová 5, 120 00 Prague

**Department of the Technology of Silicates, Institute of Chemical Technology, Suchbátarova 5, 166 28 Prague 6*

Received 23. 6. 1988

The study deals with the effect of melting temperature, sand grain size, the type and concentration of the refining agent, the size of the stagnant zone and agitation of the melt by bubbling, on the specific energy consumption and output of a model melting zone in the melting of soda-lime glass. Dissolution of sand and refining were considered as the main melting processes and the theoretical data from Part I [1] were used in the calculations. In most instances, sand dissolution was found to be the controlling process, so that the conclusions concerning the advantages of high mean melting temperatures and a small stagnant zone, reached in Part II [2], also hold in the present part. Refining controls the entire melting process only in the case of low or medium melting temperatures, and when melting batch with fine-grained sand at these temperatures. If bubbling with gas is employed, the sand dissolution and refining have to be separated in terms of space; however, even such an arrangement appears to be advantageous.

INTRODUCTION

Part II of the present study [2] included calculations of characteristics in a model melting zone, namely throughput and specific power consumption, for soda-lime sheet glass in terms of temperature, sand grain size, type and concentration of refining agent, size of the stagnant zone and mechanical mixing of the melt by bubbling. The calculations indicated above all the advantages of high melting temperatures, small stagnant zones, reducing the size of the largest sand grains and mixing the melt. Refining will also be included in the present part.

THEORETICAL AND EXPERIMENTAL

With refining included in the process, the solution represented by equations (7) through (11) in Part I [1] will hold. The equations provide the values of the mean time of residence, $\bar{\tau}$. If these values are determined or co-determined by refining, they are generally more difficult to obtain, as:

1. The values of the time of refining depend on the shape of the melting zone and on flow.
2. The required experimental values of bubble growth rate at low temperatures are merely approximate.
3. The actual size of the smallest bubbles is unknown.

The assumed critical paths of the melt and bubbles are then indicated by line BA in Fig. 2 of Part I [1].

The mean rates of bubble growth determined by earlier measurements [3, 4] were employed in calculating the time of refining. With the model glass melt (74 wt. % SiO_2, 16 wt. % Na_2O, 10 wt. % CaO) the mean values of the bubble growth rate were determined for the $As_2O_3 + NaNO_3$ refining agent at 1400 °C and 1450 °C, for Na_2SO_4 at 1470 °C and for NaCl at 1530 °C. For the sheet glass melt, the temperature dependence of the mean bubble growth rate was determined experimentally over the range of 1300 to 1550 °C [4]. The measurement of bubble growth rate at low temperatures is within the limits of the sensitivity of the method (10^{-8} — 10^{-9} m s^{-1}), so that the value established experimentally for a glass melt free of refining agents at 1400 °C was applied to glass melt containing refining agents at 1200 °C and 1250 °C. In determining the temperature dependence of the bubble growth rate for the model glass melt in the range of mean temperatures, this dependence was considered similar to that obtained experimentally with the flat glass melt. This is why the values of model characteristics of the model glass melt over the medium and lower temperature ranges should be regarded as very approximate only. The values of the mean bubble growth rates employed are listed in Table I.

Table I

Temperature dependence k (m s^{-1}) for a model glass melt refined with $As_2O_3 + NaNO_3$

% As_2O_3	Temperature, °C					
	1250	1300	1350	1400	1450	1500
0.25	5.0×10^{-9}	4.0×10^{-8}	5.0×10^{-8}	6.3×10^{-8}	9.9×10^{-8}	2.0×10^{-7}
0.5	5.0×10^{-9}	7.5×10^{-8}	1.3×10^{-7}	2.2×10^{-7}	5.8×10^{-7}	1.1×10^{-6}
1.0	5.0×10^{-9}	2.0×10^{-7}	3.8×10^{-7}	6.5×10^{-7}	1.0×10^{-6}	1.6×10^{-6}
1.5	5.0×10^{-9}	3.0×10^{-7}	5.7×10^{-7}	9.2×10^{-7}	1.4×10^{-6}	2.4×10^{-6}
2.0	5.0×10^{-9}	3.5×10^{-7}	6.7×10^{-7}	1.2×10^{-6}	1.7×10^{-6}	2.8×10^{-6}
2.5	5.0×10^{-9}	3.9×10^{-7}	7.4×10^{-7}	1.2×10^{-6}	1.8×10^{-6}	3.0×10^{-6}
3.0	5.0×10^{-9}	4.8×10^{-7}	8.2×10^{-7}	1.3×10^{-6}	2.5×10^{-6}	4.7×10^{-6}

Temperature dependence k (m s^{-1}) for float glass (0.6 % Na_2O as Na_2SO_4

t, °C	1250	1300	1350	1400	1450	1500
k (ms^{-1})	5.0×10^{-9}	2.0×10^{-8}	8.0×10^{-8}	2.4×10^{-7}	3.4×10^{-6}	1.1×10^{-5}

Further calculations of the Q and P were carried out according to equations (1—2) and (6) in the same way as in Part II [2]. The conditions for the calculations and the experimental data on sand dissolution, as well as the model equipment, were the same as those used in Part II of the present study.

Table I continued:

Temperature dependence k (m s^{-1}) for a model glass melt refined with Na_2SO_4

% Na_2O as Na_2SO_4	Temperature, °C					
	1250	1300	1350	1400	1450	1500
0.3	5.0×10^{-9}	2.0×10^{-8}	2.2×10^{-8}	3.0×10^{-8}	1.5×10^{-7}	4.7×10^{-7}
0.4	5.0×10^{-9}	2.0×10^{-8}	3.3×10^{-8}	6.7×10^{-8}	7.3×10^{-7}	2.3×10^{-6}
0.5	5.0×10^{-9}	2.0×10^{-8}	6.5×10^{-8}	1.8×10^{-7}	2.6×10^{-6}	8.0×10^{-6}
0.6	5.0×10^{-9}	2.0×10^{-8}	7.6×10^{-8}	2.3×10^{-7}	3.2×10^{-6}	1.0×10^{-5}
0.7	5.0×10^{-9}	2.0×10^{-8}	8.0×10^{-8}	2.4×10^{-7}	3.4×10^{-6}	1.1×10^{-5}
0.85	5.0×10^{-9}	2.0×10^{-8}	9.3×10^{-8}	2.8×10^{-7}	4.0×10^{-6}	1.2×10^{-5}
1.0	5.0×10^{-9}	2.0×10^{-8}	1.1×10^{-7}	3.2×10^{-7}	4.5×10^{-6}	1.4×10^{-5}

THE RESULTS OF CALCULATIONS AND THEIR DISCUSSION

The effects of accuracy of a_0 and k values on the residence time τ'_D

Figs. 1 and 2 exemplify the temperature dependence of τ'_D values for flat glass melt (Fig. 1) and for the model glass melt refined with As_2O_3 + $NaNO_3$ (Fig. 2) for three different initial bubble radii a_0. The a_0 value appears to affect very little the τ'_D over the given range. The larger the k value, the smaller the effect. No major error will therefore be introduced by choosing an arbitrary a_0 value over the assumed range of the smallest bubble size. The value $a_0 = 10^{-5}$ m was chosen for the calculation of Q and P.

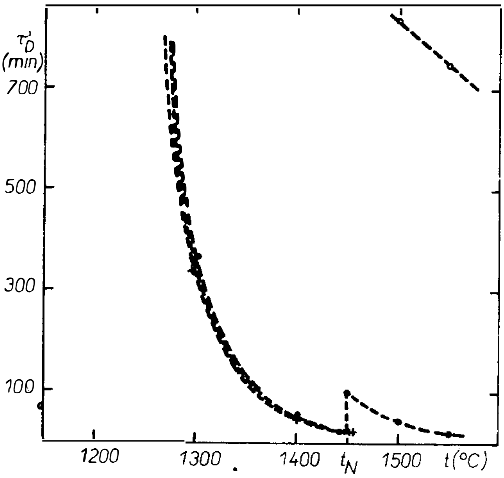

Fig. 1. Temperature dependence of τ'_D for flat glass, $r_{0\,max}$ = 0.5 mm, the mean value of k employed; ● — $a_0 = 10^{-5}$ m, × — $a_0 = 2.5 \times 10^{-5}$ m, + — $a_0 = 5 \times 10^{-5}$ m, ○ — $a_0 = 10^{-5}$, without refining agents, $k = 2.5 \times 10^{-9}$ m s^{-1}.

As demonstrated by the examples in Figs. 3 and 4, the k value influences strongly the τ'_D time, particularly over the range of low and medium temperatures. The experimental bubble growth rate values obtained in the region of medium and particularly low temperatures are of course quite inaccurate, and so are subsequently the calculated Q and P values. In view of the current dispersion of experimental bubble growth rate values, the values of k equal to one half of the mean experimental values obtained are used in the calculations (the least favourable case).

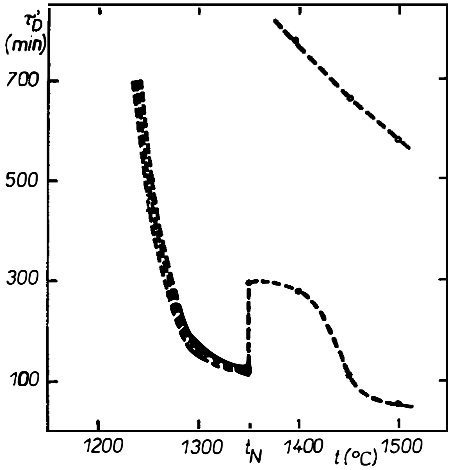

Fig. 2. Temperature dependence of τ'_D for the model glass, refining agent 0.25 % As_2O_3, $r_{0\,max}$ = *0.25 mm, the mean value of k employed,* ● — $a_0 = 10^{-5}$ m, × — $a_0 = 2.5 \times 10^{-5}$ m, + — $a_0 = 5 \times 10^{-5}$ m, o — *without refining agents,* $k = 2.5 \times 10^{-9}$ m s^{-1}.

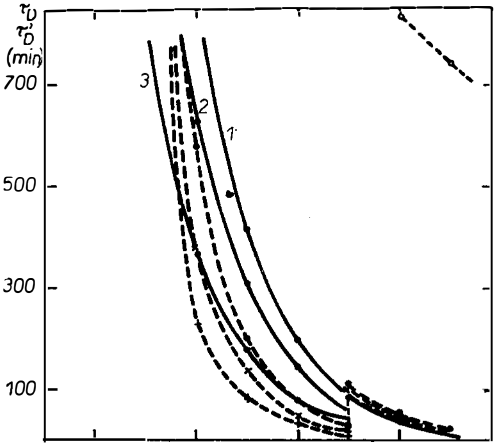

Fig. 3. Temperature dependence of τ'_D *and* τ_D *values for flat glass. The value* $r_{0\,max} = 0.5$ mm *was used in the calculation of* τ'_D; + — *k is the two-fold of the average value,* × — *k has the mean value,* ● — *k is one half of the mean value,* o — τ'_D *for the case without the refining agents,* 1 — τ_D *for* $r_{0\,max} = 0.5$ mm, 2 — τ_D *for* $r_{0\,max} = 0.4$ mm, 3 — τ_D *for* $r_{0\,max} = 0.3$ mm.

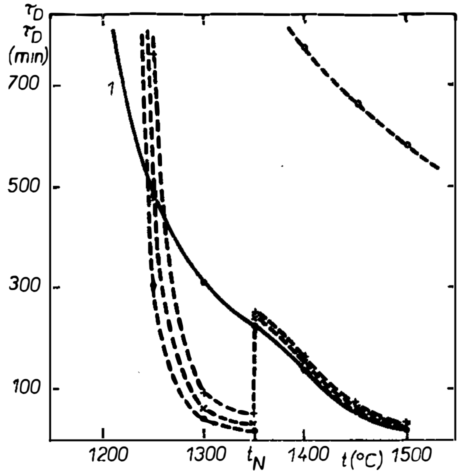

Fig. 4. Temperature dependence of τ'_D *for the model glass melt, refining agent 1* % As_2O_3 + $NaNO_3$, $r_{0\,max} = 0.25$ *mm*; + — *k is the two-fold of the mean value*, × — *k has the mean value*, • — *k is one half of the mean value*, o — τ'_D *for the case without refining agents*,

The effect of the individual factors on the residence time τ'_D if both sand dissolution and refining are considered

The effect of temperature: Similarly to sand dissolution, the τ'_D values decrease very steepely with rising temperature. Whereas at lower temperatures around the liquidus temperature the values $\tau_{D} \rightarrow \infty$, the τ'_D values are finite, but in the adjacent region of somewhat higher temperatures it frequently holds that $\tau'_D > \tau_D$, especially with finer sands (cf. Fig. 3 for $r_{0\,max} = 0.3$ mm and Figs. 5 and 6). In the mean temperature range, the decrease of τ'_D is faster than that of τ_D, so that the following holds with the exception of the finest sands: $\tau'_D < \tau_D$ (cf. Figs. 3,4 and 6). At high temperatures (above the nucleating temperature) the sum of τ_D and τ_{RN} is used in the calculation of Q and P (equation (4) and Part I). However the refining time mostly plays a less significant role, because $\tau_{RN} < \tau_D$, or even $\tau_{RN} \ll \tau_D$. If no refining agent is employed, the τ'_D values are high and decrease only slowly with increasing temperature (cf. Fig. 1—4). Under given conditions, such a case is technologically inapplicable.

The effect of the largest sand grain radius: In the case of sands with very coarse grains (cf. Fig. 3) it may hold over the entire temperature range up to the nucleation temperature that $\tau_D > \tau'_D$, while for fine sands with a low refining agent concentration (slow refining), $\tau'_D > \tau_D$ over the entire temperature range (Fig. 5). Otherwise, the points given in the paragraph above hold also for this case. Above the nucleating temperature, the τ'_D value is strongly affected by the value of $r_{0\,max}$, since, as already mentioned, τ_D is almost always larger than τ_{RN} where τ_D is proportional to $r_{0\,max}$. However, at these temperatures the τ'_D values are mostly small.

The effect of refining agent concentration: The concentration of the refining agent is given by the value k, so that, at a given temperature, the τ'_D value may

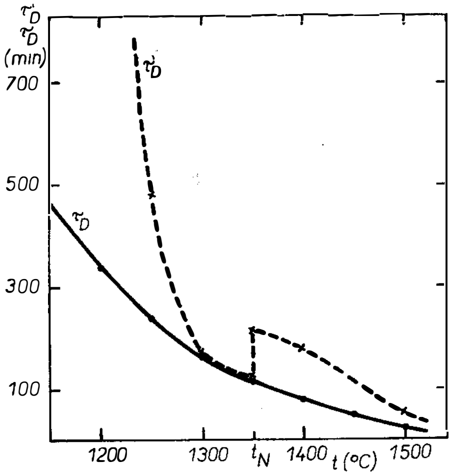

Fig. 5. Temperature dependence of τ'_D *and* τ_D *for the model glass melt, refining agent 0.25 %* $As_2O_3 + NaNO_3$, $r_{0\,max} = 0.20$ *mm, the mean value of k was used.*

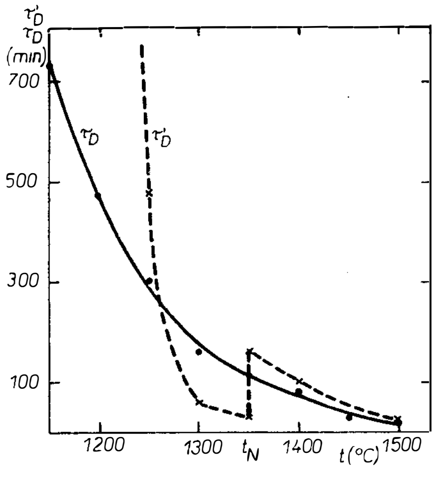

Fig. 6. Temperature dependence of τ'_D *and* τ_D *for the model glass melt, 1 %* $As_2O_3 + NaNO_3$, $r_{0\,max} = 0.20$ *mm, mean value of k was used.*

be significantly affected by this factor. As indicated by Figs. 7 and 8, this effect is strong particularly over the medium temperature range and around the nucleation temperature. At low tempertures, the *k* values decrease markedly and their size begins to be virtually independent of the refining agent concentration. At very high temperatures, the τ_{RN} values are quite small for all the refining agent concentrations. There also appears the additional effect of the τ_D and τ_{RN} sum, while in most cases $\tau_{RN} < \tau_D$. Determination of the optimum refining agent concentration is therefore significant particularly in the region of higher medium or mildly high temperatures (in the neighbourhood of the nucleation temperature).

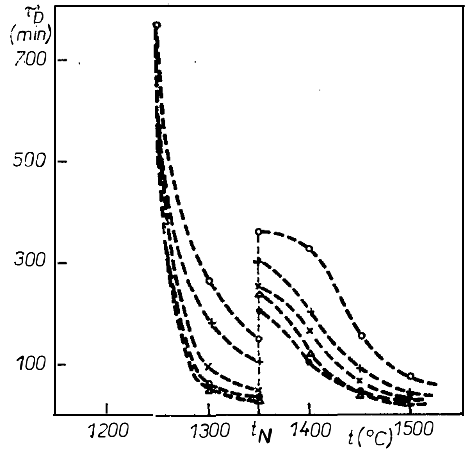

Fig. 7. Temperature dependence of τ'_D *for the model glass melt, refining agent* $As_2O_3 + NaNO_3$, $r_{0\,max}$ = *0.25 mm*; ○ — *0.25* % As_2O_3, + — *0.5* % As_2O_3, × — *1.0* % As_2O_3, ● — *2* % As_2O_3, △ — *3* % As_2O_3.

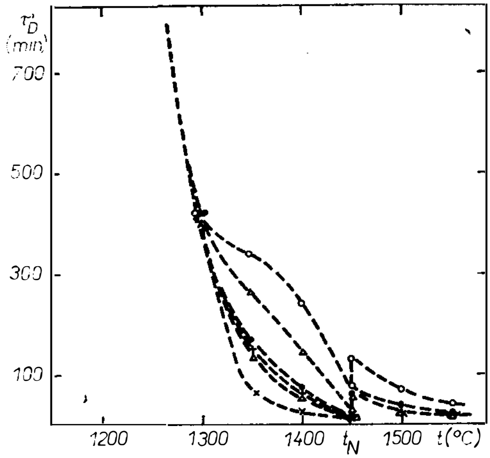

Fig. 8. Temperature dependence of τ'_D *for the model glass melt, refining agent* Na_2SO_4, $r_{0\,max}$ = *0.25 mm*; ○ — *0.3* % Na_2O *as* Na_2SO_4, △ — *0.4* % Na_2O *as* Na_2SO_4, ● — *0.5* % Na_2O *as* Na_2SO_4, + — 0.7 % Na_2O *as* Na_2SO_4, △ — *0.8* % Na_2O *as* Na_2SO_4, × — *1.0* % Na_2O *as* Na_2SO_4.

The effect of the individual factors on specific power consumption and throughput

The τ'_D values calculated for $a_0 = 10^{-5}$ m and for k equal to one half of the experimentally established bubble growth rate were compared with the τ_D values in the temperature range below the nucleation temperature, and the larger of the values compared was used in the calculation of Q and P. In the region above the nucleation temperature, direct use was made of the τ'_D value, which already includes

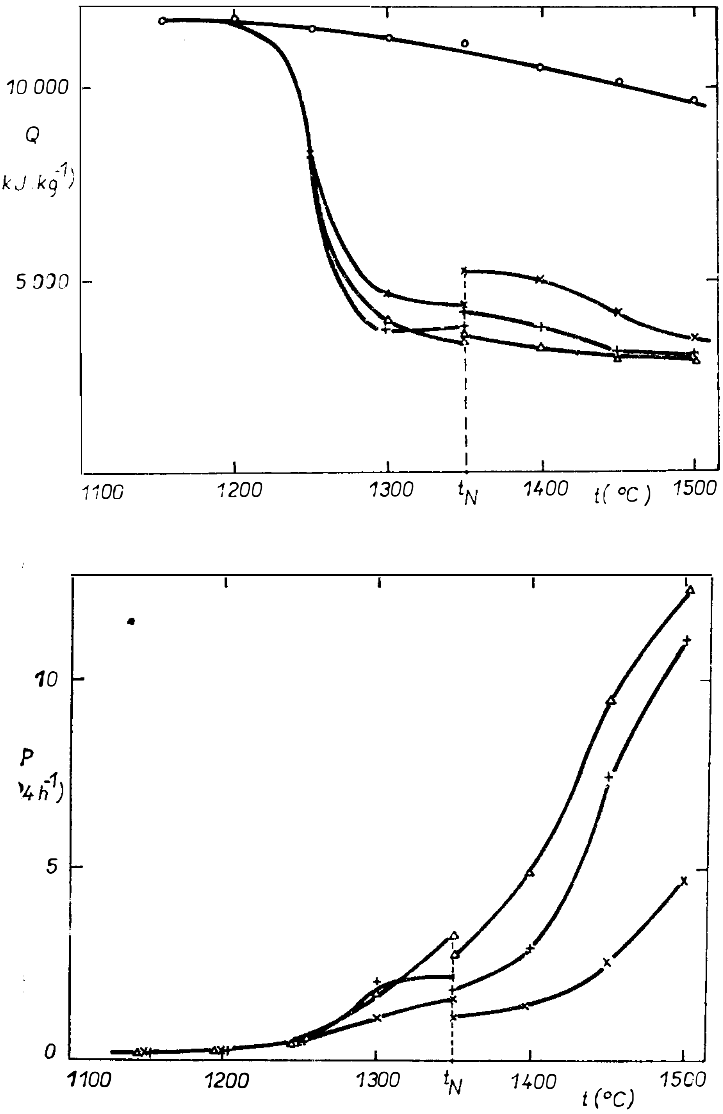

Fig. 11. Q and P till sand dissolution and refining in terms of temperature, model glass, refining agent As_2O_3 + $NaNO_3$; *m = 0.9,* $r_{0\,max}$ *= 0.20 mm,* o — *without refining agent,* × — *0.25 %* As_2O_3, + — *1.0 %* As_2O_3, △ — *2.0 %* As_2O_3.

The trends of tank throughput are the same as those in the case of sand dissolution alone.

The effect of the largest sand grain radius: Here again similar conclusions hold as for the dissolution of sand alone. Fig. 9 indicates that at lower and medium temperatures the specific power consumption is for the most part determined by sand dissolution and this is why a decrease of $r_{0\,\max}$ in this region has favourable effects. The size of $r_{0\,\max}$ does not affect the Q and P values only in the case of finer sand in the lower temperature region (cf. Fig. 9 at 1250 °C) where the melting process is controlled by refining. At high temperatures (above the nucleation temperature) the extent of losses is co-determined above all by the $r_{0\,\max}$ value. However, the losses being small, the effect on Q is likewise slight.

Fig. 9b demonstrates an increase in throughput with decreasing $r_{0\,\max}$ value over the entire temperature interval, quite in agreement with case of sand dissolution alone. As a result of heterogenous nucleation of bubbles, a discernible decrease of throughput occurs at the nucleation temperature (Figs. 9 and 11b).

The effect of refining agent concentration: There is a major difference compared to sole dissolution of sand. If the sand is coarse-grained (e.g. with flat glass), the technological time of melting at lower temperatures is controlled by sand dissolution, and in the medium and high temperature ranges the case involving both processes does not differ significantly from that of sand dissolution alone. However, a discernible difference between the two cases arises with finer sand in the low temperature region (cf. Fig. 11a). The technological time of melting is determined by refining, which is much slower than dissolution of sand, and virtually independent of refining agent concentration. In the region of medium and midly high temperatures (around the nucleation temperature) and with fine sands, the value of τ'_D, and thus also that of Q, depends significantly on the refining agent concentration, and determination of the optimum refining concentration is therefore very important. The losses are very small at very high temperatures, and the differences in the refining agent concentration hardly ever affect the specific power consumption, Q.

The throughput is affected by refining agent concentration over the temperature range of medium to high temperatures. At high temperatures, where the mean time of residence is very short, the refining agent concentration will effect the throughput considerably, but the results show very poor accuracy as a result of errors in determining the time of residence.

The effect of the stagnant zone size: The dependence of Q and P on the size of the stagnant zone for flat glass (Fig. 10) is shown as an example. At low melting temperatures, the Q value increases with increasing stagnant zone m over the entire interval of m values (for $m \to 1$, $Q \to \infty$). At high melting temperatures, Q is almost independent of this quantity over a wide range of m values, and begins to increase rapidly only from $m > 0.8-0.9$ upwards. For fine sand, the Q depends very little on this quantity over a wider range of m values in the medium temperature range (cf. Fig. 12a). As in this case the Q values are very close to the theoretical heat consumption values, this provides evidence for the advantages of a layout which would ensure the smallest possible stagnant zone size in the range of medium melting temperatures by controlling convection in the melting zone.

The throughput decreases in direct proportion to increasing m value, and the decrease is steeper at higher temperatures (cf. Figs. 10b and 12b), similarly to the case of sand dissolution alone.

This instance, decreasing the m value and choosing a suitable refining agent concentration, appears to be the most significant intensification factor besides temperature.

The effect of bubbling: Although the mixing of the glass melt by bubbling reduces the τ_D values and improves utilization of the melting zone, it dces not contribute to refining. If the bubbling process is to be utilized properly, it is neccessary to

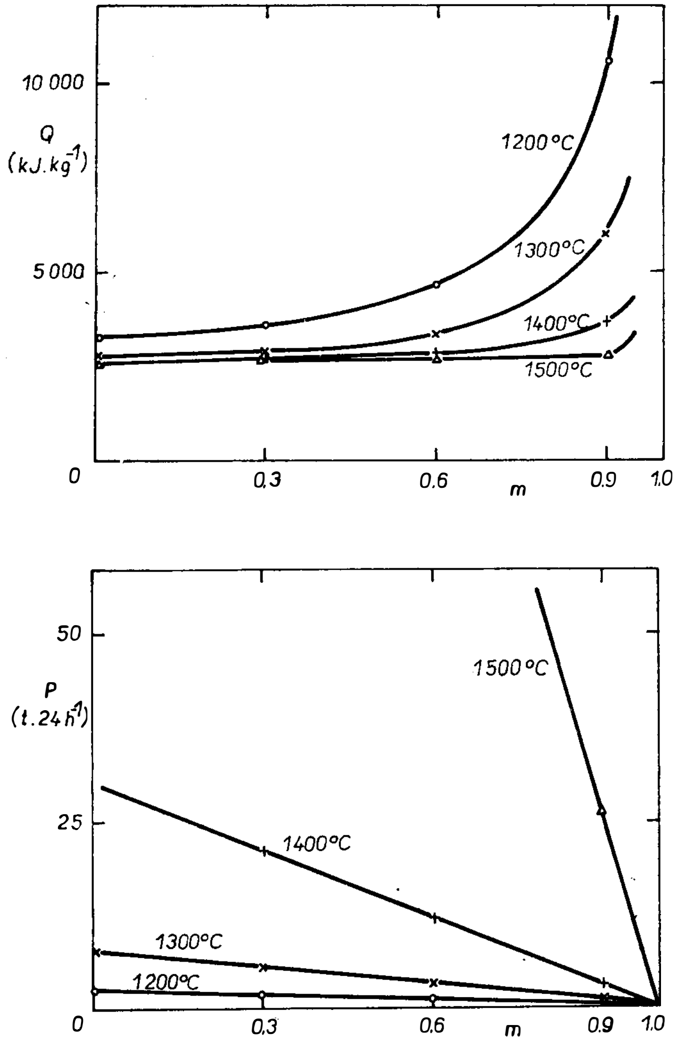

Fig. 12. Q and P till sand dissolution and refining in terms of stagnant zone m, model glass, refining agent 0.7 % Na_2O *as* Na_2SO_4, $r_{0\,max} = 0.20$ *mm.*

seek an arrangement involving dissolution of sand in the original melting zone, provided with bubbling, and refining in another zone of similar shape, separated by a barrier.

As the evaluation of the first melting zone (sand dissolution) is already known from the previous diagrams, it is possible to choose directly the advantageous variants of conditions for this zone. In the first melting zone, the suitable melting temperature should correspond to the minimum on the $Q = Q(t)$ curve, and at the same time a suitable concentration of a refining agent should ensure the fastest possible refining in the second melting zone. A high temperature should be employed in the refining melting zone ($t \geqq t_N$), to ensure a high efficiency of the refining agent.

The following equations hold for the calculation of losses in the refining zone having the same shape as the melting zone (with only the length of the former being adjusted to the requirements of refining) on the assumption of piston flow:

$$Q_{L2} = \frac{\dot{Q}_{L1}}{V_1 \varrho} \bar{\tau}_2 \frac{1}{1 - m_2} . \tag{1}$$

The $\bar{\tau}_2$ value (the time of refining) is calculated for the least favourable case, when the smallest bubble must rise from the bottom to the surface. The total specific power consumption in the second melting zone can then be calculated from the equation:

$$Q_2 = Q_{L2} + \Delta Q_M \tag{2}$$

The total specific power consumption for the entire melting area is then given by the equation:

$$Q = Q_1 + Q_2 \tag{3}$$

The dependence of the Q and P values on refining agent concentration (NaCl) is given in Fig. 13 as an example. To dissolve the sand with bubbling, the advantageous temperature of 1300 °C was chosen while the refining in the second zone proceeded at 1530 °C, since the experimental values of bubble growth rate for this temperature are known. Calculation according to equations (1) and (2) indicated that the resulting values of Q will be only little affected by the size of the stagnant zone in the second melting area, as this exhibits small specific losses (except for the case of not employing refining agents). Over a wider concentration range of the refining agent, the energy consumption in the second melting zone is generally lower by almost one order of magnitude than that in the first zone. The energy consumption in the second melting zone for the sulphate or As_2O_3 + $NaNO_3$

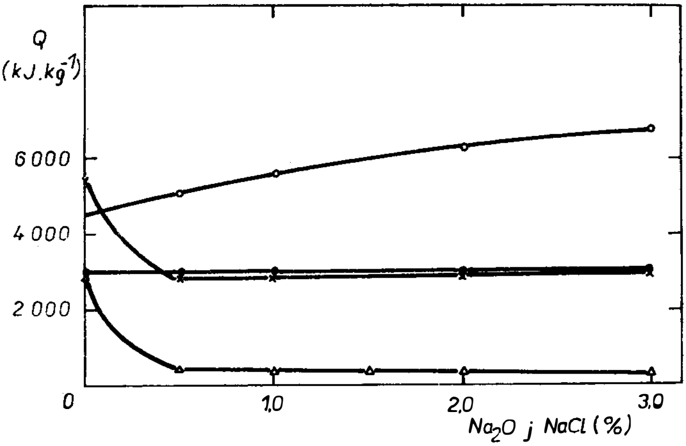

Fig. 13. Q and P in terms of NaCl *concentration, model sodalime glass,* $r_{0\,\max}$ = *0.25 mm;* *a)* ○ — *without bubbling, till sand dissolution,* m = *0.9, 1300 °C,* ● — *without bubbling till sand dissolution,* m = *0.9, 1550 °C,* × — *Q for two melting zones, bubbling and subsequent refining,* $m_1 = 0$, t_1 = *1300 °C,* ▵ — *Q for the second melting zone,* $m_2 = 0$, *1530 °C.*

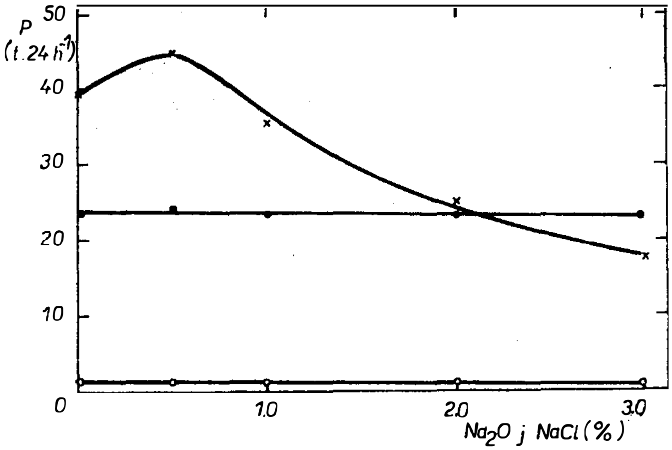

Fig. 13. b) ○ — without bubbling, 1300 °C, ● — without bubbling, 1550 °C, × — with bubbling, 2 melting zones.

refining agent and for the refining temperature of 1470 or 1450 °C, will be about 300 to 350 kJ kg^{-1}.

As indicated by Fig. 13a, the total specific power consumption for melting and refining in two separate zones corresponds roughly to sole dissolution of sand at high temperatures (without bubbling), i.e. to the case favourable from the standpoint of power conservation. A variant less advantageous from the standpoint of power consumption, i.e. melting till sand dissolution without bubbling and showing low utilization of the melting zone (an actual case) at 1300 °C, is shown in Fig. 13a for the sake of comparison.

High mean melting temperatures are technically viable in small melting furnaces and no additional intensifying measures are required. However, high mean melting temperatures cannot be attained in large tanks using classical fuel. The arrangement using controlled convection (by bubbling) would then be justified.

Fig. 13b indicates that the application of glass melt mixing and two melting zones would be advantageous even from the standpoint of the furnace throughput.

CONCLUSIONS

The results presented in the present part include the two main processes involved in the melting stage, namely dissolution of sand and refining. As has already been assumed in part II [2], the dissolution of sand is a process for the most part decisive for specific power consumptin and throughput of the furnace. One should not be led astray by the fact that bubbles and seed are the limiting factor in increasing the throughput of actual tank furnaces. High melting temperatures are advantageous with respect to sand dissolution as well as to refining; the former is of course the controlling process in most instances. The controlling effect of refining arises at low temperatures only. Refining further controls the throughput at lower and mean temperatures with fine sand and an unsuitable concentration of refining agents, or when the refining agents are not used at all. The most sensitive temperature range with respect to refining agent concentration is that close below the nucleating temperature and in its neighbourhood. Suppression of the stagnant zone appears to be a significant intensification factor, just as in the case of sand dissolution only. Appliction of bubbling requires the two main melting processes to be separated into their own melting zones, and the calculation indicates that such an arrangement could be advantageous. The power consumption of refining is lower by roughly one order than that required for sand dissolution. The results published so far indicate only the main trends in the development of the characteristics. A further work will be aimed at applying the results to actual melting zones, specifying their main parameters, and making theoretical melting conditions as close as possible to the actual ones.

References:

[1] **Němec L.: Silikáty *32,* 193 (1988).**
[2] **Němec L., Laurentová S.: Silikáty *32,* 313, (1988).**
[3] **Němec L.: Jour. Am. Ceram. Soc. *60,* 436 (1977).**
[4] **Němec L., Mühlbauer M.: Glastechn. Ber. *54,* 99 (1981).**
[5] **Němec L., Laurentová S., Freivolt Š.: Main Melting Processes with Respect to Power Consumption. Unpublished Research Report DÚ IV-4-3/04, Joint Laboratory of Silicates, Czechoslovak Academy of Sciences, and Institute of Chemical Technology, Prague (1985).**

List of symbols

a_0 — initial bubble radius (m)
k — mean bubble growth rate (m s^{-1})
m — proportion of stagnant areas in the melting zone
$r_{0\,\mathrm{max}}$ — initial effective radius of the largest sand grain in the given set (m)
t_N — temperature at which bubbles nucleate heterogeneously on sand grains (°C)
Q — specific power consumption for melting and refining (kJ kg^{-1})
Q_1 — mean power consuption in the first melting zone (kJ kg^{-1})
Q_{L2} — specific losses in refining melting zone (kJ kg^{-1})
$\dot{Q}_{L1}$ — specific energy flux through walls of the first melting zone (kJ kg^{-1} s^{-1})
Q_M — the amount of energy required for the heating of 1 kg of glass melt from melting temperature in the first melting zone to the refining temperature in the second melting zone (kJ kg^{-1})
P — the output of the melting zone (kg s^{-1})
V_1 — the volume of the first melting zone (m^3)
τ_D — the time required for dissolving the solid sand particles (s)
τ'_D — the shortest time during which the glass melt can pass over the length of the critical path if refining is employed (s)
τ_{RN} — the time required for refining heterogenously nucleated bubbles (s)
τ_2 — the mean time of residence in the second melting zone (refining time) (s)
ϱ — glass melt density

HLAVNÍ TECHNOLOGICKÉ CHARAKTERISTIKY SKLÁŘSKÝCH TAVICÍCH PROSTORŮ Z HLEDISKA PRŮBĚHU TAVICÍHO PROCESU: ČÁST III. HLAVNÍ CHARAKTERISTIKY DO OKAMŽIKU ROZPUŠTĚNÍ PÍSKU A VYČEŘENÍ

Lubomír Němec, Simona Laurentová*

Ústav chemie skelných a keramických materiálů ČSAV, 120 00 Praha
** Katedra technologie silikátů, VŠCHT, 166 28 Praha*

Měrná spotřeba energie a výkon tavicího zařízení jsou do značné míry určovány průběhem hlavních tavicích dějů — rozpouštěním písku a čeřením. V této práci byl vzhledem k průběhu obou dějů zkoumán vliv teploty, zrnitosti písku, druhu a koncentrace čeřiva, velikosti mrtvého prostoru a probublávání skloviny na tavicí charakteristiky modelového tavicího prostoru. Výsledky ukázaly, že hlavní tendence jsou podobné jako v případě, kdy uvažujeme pouze rozpouštění písku. Spotřeba energie klesá a výkon roste především se zvyšováním průměrné tavicí teploty a snižováním mrtvého prostoru. Kontrolujícím dějem je většinou rozpouštění písku. Čeření se stává kontrolujícím dějem především v oblasti nízkých a středních teplot a při použití jemnějších písků. V celém teplotním rozmezí se čeření stává kontrolujícím dějem pouze tehdy, není-li použito čeřivo; v tomto případě spotřeba energie značně narůstá a výkon klesá. Určení optimální koncentrace má největší význam v teplotní oblasti těsně pod nukleační teplotou. Použití probublávání vyžaduje rozdělení tavicího prostoru na dvě části — tavicí a čeřicí — toto uspořádání se ukazuje jako výhodné, spotřeba energie na čeření je zde zhruba o řád nižší než spotřeba na rozpouštění písku.

Obr. 1. Závislost hodnot τ'_{D} na teplotě pro plochou sklovinu, $r_{0\,\mathrm{max}} = 0{,}5$ mm, použita průměrná hodnota k;
● — $a_0 = 10^{-5}$ m,
× — $a_0 = 2{,}5 \,.\, 10^{-5}$ m,
+ — $a_0 = 5 \,.\, 10^{-5}$ m,
o — $a_0 = 10^{-5}$ m, bez čeřiv, $k = 2{,}5 \,.\, 10^{-9}$ m . s^{-1}.

Obr. 2. Závislost hodnot τ'_{D} na teplotě pro modelovou sklovinu, čeřivo 0,25 % As_2O_3, $r_{0\,\mathrm{max}} = 0{,}25$ mm, použita průměrná hodnota k;
● — $a_0 = 10^{-5}$ m,
× — $a_0 = 2{,}5 \,.\, 10^{-5}$ m,
+ — $a_0 = 5 \,.\, 10^{-5}$ m,
o — bez čeřiv, $k = 2{,}5 \,.\, 10^{-9}$ m . s^{-1}.

Obr. 3. Závislost hodnot τ'_{D} a τ_{D} na teplotě pro plochou sklovinu. Pro výpočet τ'_{D} byla použita hodnota $r_{0\,\mathrm{max}} = 0{,}5$ mm;
+ — k je dvojnásobek prům. hodnoty,
× — k má průměrnou hodnotu
● — k je polovinou průměrné hodnoty,
o — τ'_{D} pro případ bez čeřiv,
1 — τ_{D} pro $r_{0\,\mathrm{max}} = 0{,}5$ mm,
2 — τ_{D} pro $r_{0\,\mathrm{max}} = 0{,}4$ mm,
3 — τ_{D} pro $r_{0\,\mathrm{max}} = 0{,}3$ mm.

Obr. 4. Závislost hodnot τ'_{D} na teplotě pro modelovou sklovinu, čeřivo 1 % $As_2O_3 + NaNO_3$, $r_{0\,\mathrm{max}} = 0{,}25$ mm,
+ — k je dvojnásobek průměrné hodnoty,
× — k má průměrnou hodnotu
● — k je polovinou průměrné hodnoty,
o — τ'_{D} pro případ bez čeřiv.

Obr. 5. Závislost τ'_{D} a τ_{D} na teplotě pro modelovou sklovinu, čeřivo 0,25 % $As_2O_3 + NaNO_3$, $r_{0\,\mathrm{max}} = 0{,}20$ mm, použita průměrná hodnota k.

Obr. 6. Závislost hodnot τ'_{D} a τ_{D} na teplotě pro modelovou sklovinu, 1 % $As_2O_3 + NaNO_3$, $r_{0\,\mathrm{max}} = 0{,}20$ mm, použita průměrná hodnota k.

Obr. 7. Závislost hodnot τ'_{D} na teplotě pro modelovou sklovinu, čeřivo $As_2O_3 + NaNO_3$, $r_{0\,\mathrm{max}} = 0{,}25$ mm;
o — 0,25 % As_2O_3, ● — 2 % As_2O_3,
+ — 0,5 % As_2O_3, △ — 3 % As_2O_3.
× — 1,0 % As_2O_3.

Obr. 8. Závislost hodnot τ'_D *na teplotě pro modelovou sklovinu, čeřivo* Na_2SO_4, $r_{0\,max} = 0{,}25$ *mm*;
○ — 0,3 % Na_2O *j.* Na_2SO_4, + — *0,7* % Na_2O *j.* Na_2SO_4,
△ — *0,4* % Na_2O *j.* Na_2SO_4, △ — *0,8* % Na_2O *j.* Na_2SO_4,
● — *0,5* % Na_2O *j.* Na_2SO_4, × — *1,0* % Na_2O *j.* Na_2SO_4.

Obr. 9. Q a P do rozpuštění písku a vyčeření v závislosti na teplotě, plochá sklovina, m = 0,9;
● — $r_{0\,max} = 0{,}6$ *mm*, × — $r_{0\,max} = 0{,}3$ *mm*,
○ — $r_{0\,max} = 0{,}5$ *mm*, + — $r_{0\,max} = 0{,}3$ *mm*.

Obr. 10. Q a P do rozpuštění písku a vyčeření v závislosti na mrtvém prostoru m, plochá sklovina, $r_{0\,max} = 0{,}5$ *mm.*

Obr. 11. Q a P do rozpuštění písku a vyčeření v závislosti na teplotě, modelová sklovina, čeřivo $As_2O_3 + NaNO_3$, *m = 0,9*, $r_{0\,max} = 0{,}20$ *mm*;
○ — *bez čeřiv*, + — *1,0* % As_2O_3,
× — *0,25* % As_2O_3, △ — *2,0* % As_2O_3.

Obr. 12. Q a P do rozpuštění písku a vyčeření v závislosti na mrtvém prostoru m, modelová sklovina, čeřivo 0,7 % Na_2O *j.* Na_2SO_4, $r_{0\,max} = 0{,}20$ *mm.*

Obr. 13. Q a P v závislosti na koncentraci NaCl, *modelová sodnovápenatá sklovina*, $r_{0\,max} = 0{,}25$ *mm*;
a) ○ — *bez probublávání do rozp. písku, m = 0,9, 1300 °C,*
● — *bez probublávání do rozp. písku, m = 0,9, 1550 °C*
× — *Q pro dva tavicí prostory, probublávání a násl. čeření,* $m_1 = 0$, $t_1 = 1300$ *°C,*
△ — *Q pro druhý tavicí prostor,* $m_2 = 0$, *1530 °C*;
b) ○ — *bez probublávání, 1300 °C,*
● — *bez probublávání, 1550 °C,*
× — *s probubláváním, 2 tavicí prostory.*

ОСНОВНЫЕ ТЕХНОЛОГИЧЕСКИЕ ХАРАКТЕРИСТИКИ СТЕКЛОПЛАВИЛЬНЫХ ПРОСТРАНСТВ С ТОЧКИ ЗРЕНИЯ ХОДА ПЛАВИЛЬНОГО ПРОЦЕССА III. ОСНОВНЫЕ ХАРАКТЕРИСТИКИ ДО МОМЕНТА РАСТВОРЕНИЯ ПЕСКА И ОСВЕТЛЕНИЯ

Лубомир Немец, Симона Лаурентова*

Институт химии стекольных и керамических материалов ЧСАН, 120 00 Прага
**кафедра технологии силикатов Химико-технологического института, 166 28 Прага*

Удельный расход энергии и мощность плавильной установки до значительной степени определяются ходом основных плавильных процессов — растворением песка и осветлением. В предлагаемой работе, имея в виду ход обоих процессов, авторами исследуются влияние температуры, гранулометрический состав песка, вида и концентрация осветлителя, размера мертвого пространства и барботирования стекломассы на характеристики плавления модельного плавильного пространства. Результаты показали, что основные тенденции подобны как в случае, когда учитывается только растворение песка. Расход энергии понижается и мощность растет прежде всего с повышением средней температуры плавления и понижением мертвого пространства. Контролирующим процессом в большинстве случаев является растворение песка. Осветление становится контролирующим процессом прежде всего в области низких и средних температур и при применении песков с низким гранулометрическим составом. В целом температурном диапазоне осветление становится контролирующим процессом только тогда, когда не применяется осветлитель. В таком случае расход энергии значительно нарастает и мощность понижается. Установление оптимальной концентрации имеет наибольшее значение в температурном диапазоне незначительно ниже температуры нуклеации. Применение барботажа требует разделение плавильного процесса на две части — часть плавления и часть осветления. Приводимое упорядочение оказывается наиболее пригодным, расход энергии на осветление приблизительно на порядок ниже, чем расход на растворение песка.

Рис. 1. Зависимость величин τ'_D *от температуры в случае листовой стекломассы,* $r_{0\,макс} = 0{,}5$ *мм, при применении средней величины к*; ● — $a_0 = 10^{-5}$ *м*, × — $a_0 = 2{,}5 \cdot 10^{-5}$ *м*, + — $a_0 = 5 \cdot 10^{-5}$ *м*, о — $a_0 = 10^{-5}$ *м, без осветлителя, к* $= 2{,}5 \cdot 10^{-9} \cdot c^{-1}$.

Рис. 2. Зависимость величин τ'_D *от температуры для модельной стекломассы, осветлитель 0,25 %* As_2O_3, r_0 макс *= 0,25 мм, при применении средней величины к;* ● *—* $a_0 = 10^{-5}$ *м, + —* $a_0 = 5 \cdot 10^{-5}$ *м,* ○ *— без осветлителей, к = 2,5 .* 10^{-9} *м . .* c^{-1}.

Рис. 3. Зависимость величин τ'_D *и* τ_D *от температуры в случае листовой стекломассы. Для расчета* τ'_D *применяли величину* r_0 макс *= 0,5 мм; + — к = двойное количество средней величины, x — к имеет среднюю величину,* ● *— к = половина средней величины,* ○ *—* τ'_D *в случае без применения осветлителей, 1 —* τ_D *для* r_0 макс *= 0,5 мм, 2 —* τ_D *для* r_0 макс *= 0,4 мм, 3 —* τ_D *для* r_0 макс *= 0,3 мм.*

Рис. 4. Зависимость величин τ'_D *от температуры для модельной стекломассы, осветлитель 1 %* $As_2O_3 + NaNO_3$, r_0 макс *= 0,25 мм; + — к = двойное колисество средней величлны, × — к = половина средней величлны,* ○ *—* τ'_D *в случае без применения осветлителей.*

Рис. 5. Зависимость τ'_D *и* τ_D *от температуры для модельной стекломассы, осветлитель 0,25 %* $As_2O_3 + NaNO_3$, r_0 макс *= 0,20 мм, с применением средней величины к.*

Рис. 6. Зависимость величин τ'_D *и* τ_D *от температуры для модельной стекломассы, 1 %* $As_2O_3 + NaNO_3$, r_0 макс *= 0,20 мм, с применением средней величины к.*

Рис. 7. Зависимость величин τ'_D *от темрературы для модельной стекломассы, осветлитель* $As_2O_3 + NaNO_3$, r_0 макс *= 0,25 мм;* ○ *— 0,25* As_2O_3, *+ — 0,5* As_2O_3, *× — 1,0 %* As_2O_3, ● *— 2 %* As_2O_3, ▵ *— 3 %* As_2O_3.

Рис. 8. Зависимость величин τ'_D *от температуры для модельной стекломассы, осветлитель* Na_2SO_4, r_0 макс *= 0,25 мм;* ○ *— 0,3 %* Na_2O *к.* Na_2SO_4, ▲ *— 0,4 %* Na_2O *к.* Na_2SO_4, ● *— 0,5 %* Na_2O *к.* Na_2SO_4, *+ — 0,7 %* Na_2O *к.* Na_2SO_4, ▵ *— 0,8 %* Na_2O *к.* Na_2SO_4, *× — 1,0 % к.* Na_2SO_4.

Рис. 9. Q и P до растворения песка и осветления в зависимости от температуры. листовая стекломасса, m = 0,9; ● *—* r_0макс *= 0,6 мм,* ○ *—* r_0 макс *= 0,5 мм, × —* r_0 макс *= 0,5 мм, + —* r_0 макс *= 0,3 мм.*

Рис. 10. Q и P до растворения песка и осветления в зависимости от мертвого пространства m, листовая стекломасса, r_0 макс *= 0,3 мм.*

Рис. 11. Q и P до растворения песка и осветления в зависимости от температуры, модельная стекломасса, осветлитель $As_2O_3 + NaNO_3$, *m = 0,9,* r_0 макс *= 0,20 мм;* ○ *— безосветлителей, × — 0,25 %* As_2O_3, *+ — 1,0 %* As_2O_3, ▵ *— 2,0 %* As_2O_3.

Рис. 12. Q и P до растворения песка и осветления в зависимости от мертвого пространства m, модельная стекломасса, осветлитель 0,7 % Na_2O *к.* Na_2SO_4, r_0 макс *= = 0,20 мм.*

Рис. 13. Q и P в зависимости от концентрации NaCl, *модельная натриевокальциевая стекломасса,* r_0 макс *= 0,25 мм; а)* ○ *— без барботирования до растворения песка, m = 0,9, 1300 °C,* ● *— без барботирования до растворения песка, m = 0,9, 1550 °C, x — Q для двух плавильных пространств, барботирование и последующее осветление,* $m_1 = 0$, $t_1 = 1300$ *°C,* ▵ *— Q для второго плавильного пространства,* $m_2 = 0$, *1530 °C; ь)* ○ *— без барботирования, 1300 °C,* ● *— без барботирования, 1550 °C, x — с барботированием, 2 плавильных пространства*

KOORDINACE ČINNOSTI V OBLASTI VÝZKUMU SUPRAVODIČŮ V ZÁPADNÍ EVROPĚ. V oblasti supravodičů dochází v Evropě k horečné činnosti. Pro její usměrnění přijaly instituce odpovědné v jednotlivých zemích za výzkum, a to západoněmecké Deutsche Forschungsgemeinschaft a Max-Planck-Gesellschaft zur Förderung der Wissenschaften, francouzský Centre National de la Recherche Scientifique, italský Consiglio Nazionale delle Ricerche a britský Science and Engineering Research Council, některá opatření. Patří mezi ně:

— výměna informací o národních výzkumných programech a způsobu jejich financování,
— výměna informací o jednotlivých specialistech a zařízení,
— organizování společných laboratoří,
— poskytování zahraničních stipendií,
— výměna výsledků výzkumu před jejich publikováním a
— zahájení celoevropských výzkumných projektů se stanovenými účastnickými vklady.

Zárukou provádění těchto opatření bude stálý výbor složený ze zástupců zúčastněných zemí. Očekává se, že k tomuto dění se připojí i vědecké instituce Švýcarska a Holandska.

Interceram 1988, č. 3, 40

Doušková